Stem Cell Research 56 (2021) 102526

Contents lists available at ScienceDirect

Stem Cell Research

journal homepage: www.elsevier.com/locate/scr

Lab Resource: Multiple Cell Lines

Generation of multiple human iPSC lines from peripheral blood mononuclear cells of two *SLC2A3* deletion and two *SLC2A3* duplication carriers

Georg C. Ziegler [a,b,*], Franziska Radtke [c], Maria Rosaria Vitale [a,g], André Preuße [a], Eva Klopocki [d], Stefan Herms [e,f], Klaus-Peter Lesch [a,g,h]

[a] Division of Molecular Psychiatry, Center of Mental Health, University of Würzburg, Würzburg, Germany
[b] Department of Psychiatry, Psychosomatics and Psychotherapy, University Hospital Würzburg, Würzburg, Germany
[c] Department of Child and Adolescent Psychiatry, Psychosomatics and Psychotherapy, University Hospital Würzburg, Würzburg, Germany
[d] Institute of Human Genetics, Biocentre, University of Würzburg, Würzburg, Germany
[e] Institute of Human Genetics and Department of Genomics, Life and Brain Center, University of Bonn, Bonn, Germany
[f] Human Genomics Research Group, Department of Biomedicine, University Hospital Basel, Basel, Switzerland
[g] Laboratory of Psychiatric Neurobiology, Institute of Molecular Medicine, I.M. Sechenov First Moscow State Medical University, Moscow, Russia
[h] Department of Psychiatry and Neurobiology, School for Mental Health and Neuroscience (MHeNs), Maastricht University, Maastricht, the Netherlands

A B S T R A C T

Copy number variants of *SLC2A3,* which encodes the glucose transporter GLUT3, are associated with several neuropsychiatric and cardiac diseases. Here, we report the successful reprogramming of peripheral blood mononuclear cells from two *SLC2A3* duplication and two *SLC2A3* deletion carriers and subsequent generation of two transgene-free iPSC clones per donor by Sendai viral transduction. All eight clones represent bona fide hiPSCs with high expression of pluripotency genes, ability to differentiate into cells of all three germ layers and normal karyotype. The generated cell lines will be helpful to enlighten the role of glucometabolic alterations in pathophysiological processes shared across organ boundaries.

1. Resource Table:

Unique stem cell lines identifier	UKWMPi007-A, UKWMPi007-B, UKWMPi008-A, UKWMPi008-B, UKWMPi011-A, UKWMPi011-B, UKWMPi012-A, UKWMPi012-B
Alternative names of stem cell lines	bCJ9cl1 (UKWMPi007-A), bCJ9cl3 (UKWMPi007-B), bCJ10cl2 (UKWMPi008-A), bCJ10cl6 (UKWMPi008-B), bCJ13cl3 (UKWMPi011-A), bCJ13cl5 (UKWMPi011-B), bCJ14cl1 (UKWMPi012-A), bCJ14cl2 (UKWMPi012-B)
Institution	Division of Molecular Psychiatry, Center of Mental Health, University Hospital Würzburg, Germany
Contact information of distributor	Georg C. Ziegler, ziegler_g@ukw.de
Type of cell lines	iPSC
Origin	human
Additional origin and disease info	UKWMPi007, Age: 77, Sex: Male, Ethnicity: Caucasian, apparently healthy
	UKWMPi008, Age: 36, Sex: Female, Ethnicity: Caucasian, apparently healthy
	UKWMPi011, Age: 41, Sex: Female, Ethnicity: Caucasian, attention-deficit/hyperactivity disorder (ADHD)
	UKWMPi012, Age: 54, Sex: Male, Ethnicity: Caucasian, attention-deficit/hyperactivity disorder (ADHD)
Cell Source	Total PBMCs
Clonality	Clonal
Method of reprogramming	Non-integrative Sendai virus
Genetic Modification	No
Type of Genetic Modification	N/A
Evidence of the reprogramming transgene loss	RT-PCR
Gene/locus	UKWMPi007-A and B: chr. 12: 8005624–8109412, 1 copy variant
	UKWMPi008-A and B: chr. 12: 8005624–8130958, 1 copy variant
	UKWMPi011-A and B: chr. 12: 8005624–8105015, 3 copy variant

(continued on next column)

(continued)

(continued on next page)

* Corresponding author.

https://doi.org/10.1016/j.scr.2021.102526
Received 13 August 2021; Accepted 29 August 2021
Available online 1 September 2021

(*continued*)

	UKWMPi012-A and B: chr. 12: 7989403–8105015, 3 copy variant (data from QuantiSNP software) Assembly: GRCh37, hg19. All CNVs comprise the whole *SLC2A3* gene (ENSG00000059804, chr. 12: 8071826–8088871), *NANOGP1* (ENSG00000176654, chr. 12: 8045172–8052736), and at least the first translated exon of *SLC2A14* (ENSG00000173262, chr. 12: 7965108–8043744).
Date archived/stock date	UKWMPi007-A and B: 08/2019 UKWMPi008-A and B: 09/2019 UKWMPi011-A and B: 12/2019 UKWMPi012-A and B: 12/2019
Cell line repository/bank	hPSCreg https://hpscreg.eu/cell-line/UKWMPi007-A https://hpscreg.eu/cell-line/UKWMPi007-B https://hpscreg.eu/cell-line/UKWMPi008-A https://hpscreg.eu/cell-line/UKWMPi008-B https://hpscreg.eu/cell-line/UKWMPi011-A https://hpscreg.eu/cell-line/UKWMPi011-B https://hpscreg.eu/cell-line/UKWMPi012-A https://hpscreg.eu/cell-line/UKWMPi012-B
Ethical approval	Ethics Committee, Medical Faculty, University of Würzburg, Ethical approval number 96/11

1.1. Resource utility

The glucose transporter GLUT3 (*SLC2A3*) provides energy for axonal outgrowth and neurotransmitter release and is highly expressed in fetal cardiomyocytes. Hence, iPSC lines carrying *SLC2A3* copy number variants (CNVs) will potentially contribute to a better understanding of glucometabolic processes in brain and heart development and degeneration (Ziegler et al., 2020).

2. Resource details

Several studies have associated common *SLC2A3* CNVs with attention-deficit/hyperactivity disorder (ADHD) (Merker et al., 2017), age of onset of Huntington's disease (Vittori et al., 2014), and congenital heart defects in patients with 22q11.2 microdeletion (Mlynarski et al. 2015) and Turner syndrome (Prakash et al., 2016). We hypothesized that these associations are due to an energetic dysregulation during glucose-sensitive developmental stages ultimately promoting metabolic stress and degenerative processes (Ziegler et al., 2020). However, there is a lack of experimental human studies, which address the impact of *SLC2A3* CNVs at the cellular level. We therefore generated two iPSC clones each from two *SLC2A3* deletion carriers (both apparently healthy, female, 36 years old, and male, 77 years old) and two *SLC2A3* duplication carriers (both with adult ADHD, female, 41 years old, and male, 54 years old), respectively. The CNVs on chr. 12p13.31 comprise the whole *SLC2A3* gene as well as the pseudogene *NANOGP1,* and at least the first exon of *SLC2A14* (ENSG00000173262).

In brief, peripheral blood mononuclear cells (PBMCs) were reprogrammed with the CytoTune-iPS Reprogramming Kit 2.0 (Thermo Fisher). Colonies with typical iPSC-like appearance (Fig. 1**A**) were picked and expanded under feeder-free conditions (37 °C, 5% CO_2) with splitting steps (ratio 1:8) every 3 to 4 days by Accutase (Merck Millipore) and Rock inhibitor treatment (10 μM Y27632, Miltenyi Biotech) for 24 h after passaging or thawing. All cell lines showed typical iPSC morphology forming dense, sharp-edged colonies (Fig. 1**A**). Positive immunostainings for OCT3, SSEA4, and TRA-1–60 proved the expression of pluripotency markers (Fig. 1**B**). Additionally, all eight iPSC lines formed embryoid bodies (EBs) in serum-containing medium (Fig. 1**C**), and cells of all three germ layers developed within these EBs after 4 weeks of cultivation in adherent conditions as indicated by positive immunostainings for α-SMA (mesoderm), AFP (endoderm), and βIII-Tubulin (ectoderm) (Fig. 1**D**). qRT-PCR showed a marked increase in expression of the pluripotency genes *REX1*, *SOX2*, *LIN28A*, and *OCT3* as compared to non-reprogrammed PBMCs (Fig. 1**E**). *SLC2A3* duplication and deletion variants were confirmed by TaqMan® CNV assay Hs_00406005 (Thermo Fisher) (Fig. 1**F**) and by means of the Illumina Infinium Global Screening Array v3.0. Standard G-banding and molecular karyotyping revealed normal karyotypes without evidence for structural or numerical chromosome aberrations (Fig. S1**A**). Absence of Sendai-viral transcripts SeV, c-Myc, Klf4, and KOS was confirmed by RT-PCR and gel-electrophoresis (Fig. S1**B**). All cell lines were free of Mycoplasma (Fig. S1**C**). Genetic identity of all cell lines with respective donor DNA extracted from blood was checked by genotype fingerprinting. All investigations were performed around passage 10.

Taken together, we generated four iPSC lines with a heterozygous *SLC2A3* deletion, and four iPSC lines carrying an *SLC2A3* gain (3 copies), which all show expression of pluripotency markers, differentiate spontaneously into cells of all three germ layers, and are karyotypically normal. Thus, our *SLC2A3* CNV iPSC lines are a suitable cellular model to study the effects of *SLC2A3* gene-dosage dependent cellular alterations on the pathophysiology of a wide range of diseases, comprising developmental and degenerative neuropsychiatric and cardiovascular diseases.

3. Materials and methods

3.1. PBMC isolation

PBMCs were extracted from EDTA blood by Ficoll density gradient centrifugation and cultivated in suspension for 4 days in StemPro-34 SFM (Thermo Fisher) with 100 ng/ml SCF, 100 ng/ml FLT-3, 20 ng/ml IL-3, and 20 ng/ml IL-6 (all Peprotech).

3.2. Reprogramming of PBMCs into iPSCS

PBMCs were reprogrammed by transduction with Sendai virus particles carrying KOS, hc-Myc, and hKlf4 for 24 h (CytoTune-iPSC Reprogramming Kit 2.0, Thermo Fisher). After 3 days, cells were transferred to Matrigel™ (Corning)-coated 6 well plates and kept in adherent culture henceforth. On day 7, PBMC medium was exchanged for StemMACS™ iPS BrewXF (Miltenyi Biotec). In the third week after transduction colonies displaying typical iPSC morphology were picked and further expanded.

3.3. Germ layer differentiation

IPSCs were seeded on ultra-low attachment plates (Corning) in differentiation medium (DMEM, 10% FBS, 1% NEAA, 100 μM β-mercaptoethanol). After 5 days, EBs were plated on 0.1% gelatine (PAN Biotech)-coated plates to facilitate differentiation. Immunofluorescence analysis was carried out after 4 weeks.

3.4. Immunofluorescence analysis

Cells were fixed with 4% paraformaldehyde (Roth). Unspecific binding was blocked by 5% FBS and 1% BSA in PBS. For intracellular targets, cells were permeabilized with 0.2% Triton X-100 for 30 min at RT. For TRA-1–60 and SSEA4 cells were stained without permeabilization. Primary antibodies (Table 2) were incubated overnight at 4 °C, and secondary antibodies (Table 2), and DAPI (300 nM, Sigma) for 1 h at RT. Staining patterns were visualized by an inverted fluorescence microscope (Olympus).

3.5. qRT-PCR

Total RNA was extracted from iPSCs (Qiagen kit), and RNA was reverse-transcribed by QuantiTect® Reverse Transcription Kit (Qiagen). The reaction was run with SYBR™ Select Master Mix (Thermo Fisher) in a CFX384 thermocycler (Biorad). Data analysis was performed with qbase^{+} software.

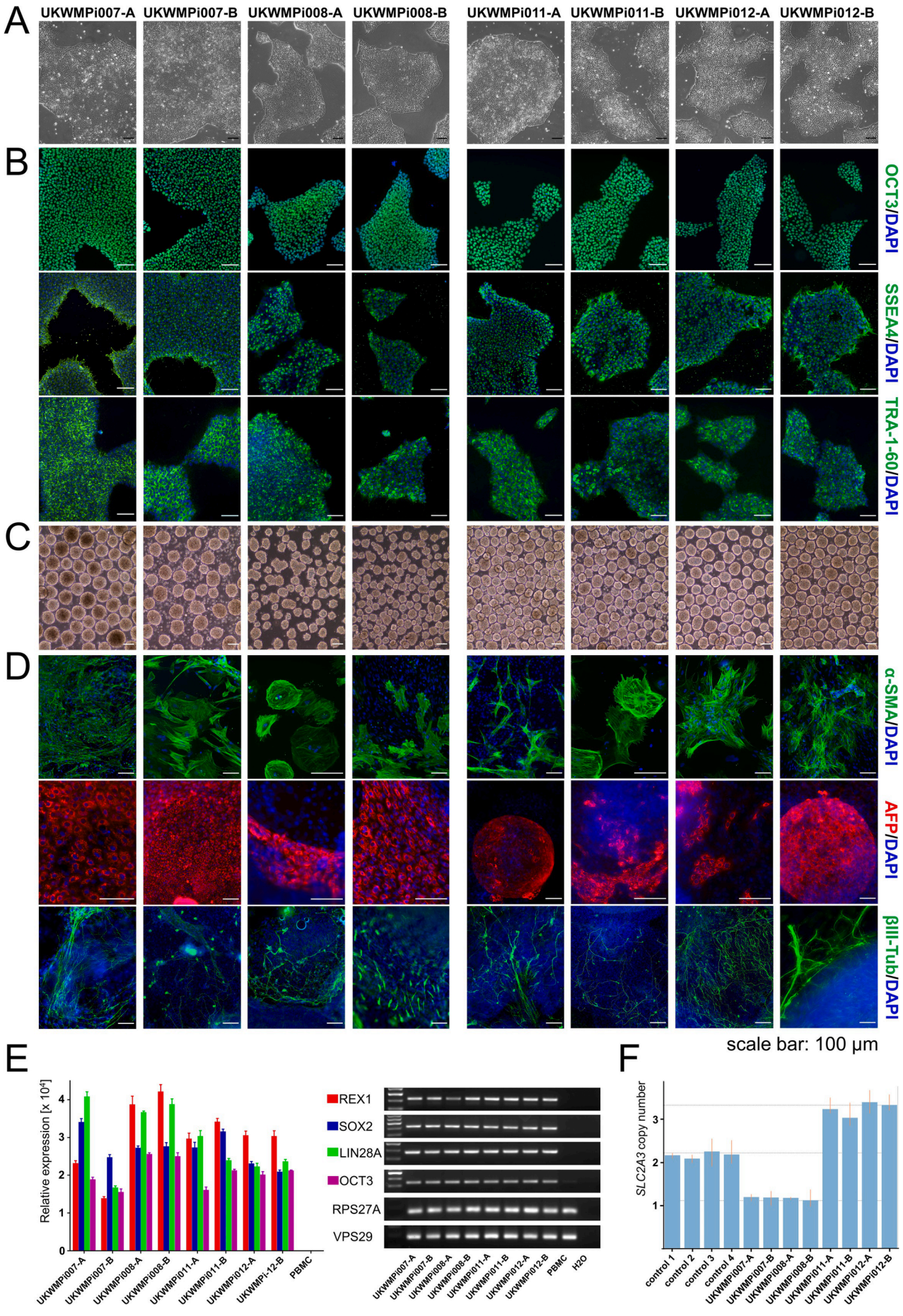

(caption on next page)

Fig. 1. Characterization of iPSC lines (A-F). **A** Morphology of iPSC colonies. **B** Immunostainings of pluripotency marker proteins. **C** Embryoid bodies. **D** Immunostainings of mesodermal (α-SMA), endodermal (AFP), and ectodermal (βIII-Tub) marker proteins. **E** Relative mRNA expression levels of pluripotency marker genes in the iPSC lines compared to PBMCs. **F** Calculation of *SLC2A3* copy number from TaqMan CNV assay data.

Table 1
Characterization and validation.

Classification	Test	Result	Data
Morphology	Light microscopy, Phase contrast	hESC-like morphology	Fig. 1A
Phenotype	Qualitative analysis	Expression of pluripotency markers OCT3, SSEA4, TRA-1–60	Fig. 1B
	Quantitative analysis (qRT-PCR)	*REX1*, *SOX2*, *LIN28A*, and OCT3: positive	Fig. 1E
Genotype	Karyotype (G-banding) and resolution	UKWMPi007-A: 46, XY (400) UKWMPi007-B: 46, XY (400) UKWMPi008-A: 46, XX (400) UKWMPi008-B: 46, XX (400) UKWMPi011-A: 46, XX (400) UKWMPi011-B: 46, XX (400) UKWMPi012-A: 46, XY (500) UKWMPi012-B: 46, XY (500)	Fig. S1A Findings submitted in archive with journal
Identity	Illumina Infinium Global Screening Array v3.0. SNP fingerprinting		Available with authors
Mutation analysis	TaqMan® CNV assay Hs_00406005 (Thermo Fisher)	UKWMPi007-A and B: 1 copy UKWMPi008-A and B: 1 copy UKWMPi011-A and B: 3 copies UKWMPi012-A and B: 3 copies	Fig. 1F
Microbiology and virology	Mycoplasma	LookOut(R) Mycoplasma PCR Detection Kit: negative	Fig. S1C
Differentiation potential	Embryoid body formation and undirected differentiation	Expression of α-smooth muscle actin, α-feto protein, and βIII-Tubulin	Fig. 1B
Donor screening	HIV 1 + 2, Hepatitis B, Hepatitis C	Negative	Submitted in archive with journal
Genotype additional info	Blood group genotyping	N/A	N/A
	HLA tissue typing	N/A	N/A

Table 2
Reagents details.

	Antibodies used for immunocytochemistry/flow-cytometry			
	Antibody	Dilution	Company Cat #	RRID
Pluripotency Markers	Mouse anti-OCT3	1:50	Santa Cruz, Cat# sc5279	AB_628051
	Mouse anti-SSEA4	1:200	Thermo Fisher, Cat# MA1-021	AB_2536687
	Mouse anti-TRA-1–60	1:50	Santa Cruz, Cat# Sc21705	AB_628385
Differentiation Markers	Mouse anti-α-SMA	1:1000	R&D, Cat#MAB1420	AB262054
	Rabbit anti-AFP	1:1000	Dako, Cat# A0008	AB_2650473
	Mouse anti-βIII Tubulin	1:1000	Promega, Cat# G7121	AB_430874
Secondary antibodies	Goat Anti-Rabbit 555	1:400	Thermo Fisher, Cat# A11034,	AB_2576217
	Goat Anti-Mouse488	1:400	Thermo Fisher, Cat# A11029,	AB_138404
	Primers			
	Target	Size of band	Forward/Reverse primer (5′-3′)	
Sendai virus detection (RT-PCR)	SeV	181 bp	GGATCACTAGGTGATATCGAGC/ACCAGACAAGAGTTTAAGAGATATGTATC	
	KOS	528 bp	ATGCACCGCTACGACGTGAGCGC/ACCTTGACAATCCTGATGTGG	
	Klf4	410 bp	TTCCTGCATGCCAGAGGAGCCC/AATGTATCGAAGGTGCTCAA	
	c-Myc	532 bp	TAACTGACTAGCAGGCTTGTCG/TCCACATACAGTCCTGGATGATGAT	
Pluripotency Markers (qRT-PCR)	*REX1*	162 bp	AGGTGGCATTGGAAATAGCAGA/AGTGGGGTGGGTTTGCCTA	
	SOX2	160 bp	GACAGTTACGCGCACATGAA/TCATGGAGTTGTACTGCAGGG	
	LIN28A	136 bp	CTGTAAGTGGTTCAACGTGCG/CTTCAAGCTCCGGAACCCTT	
	OCT3	119 bp	CCCACACTGCAGCAGATCA/TGTGCATAGTCGCTGCTTGA	
Reference genes (qRT-PCR)	*PSMB4*	140 bp	GGACATGCTTGGTGTAGCCT/AGCGTTCTACTAAGTCGCGG	
	RPS27A	79 bp	GGTTAAGCTGGCTGTCCTGAA/AGAAGGGCACTCTCGACGAA	
	VPS29	146 bp	GACTCTGGCTGGTGATGTTCA/AGCTGGCCATATCTCCCCAT	

3.6. TaqMan genotyping assay

10 ng genomic DNA, 5 μl TaqMan genotyping master mix, 0.5 μl TaqMan copy number reference assay, 0.5 μl TaqMan SLC2A3 assay (Hs_00406005, all reagents Thermo Fisher), and 5 μl H2O were mixed. The reaction was run in quadruplicates in a BioRad CFX 384 cycler (10 min. 95 °C, followed by 40 cycles of 15 s at 95 °C and 60 s at 60 °C). Data were analyzed by CopyCaller™ software (Fig. 1 F).

3.7. Karyotype analysis

Karyotyping was performed by GTG-banding and analysis of at least 11 metaphases by the Institute of Human genetics, University of Würzburg. All samples were examined with a resolution of 400–500 bands (Table 1) by using an Axioskop (Zeiss) microscope.

3.8. Molecular karyotyping and SNP fingerprinting analysis

Genomic DNA was processed on Global Screening Array v3.0 (GSAMD24v3-0, Illumina, Inc. San Diego) by the Institute of Human Genetics, LIFE&BRAIN GmbH, University of Bonn. SNP calling was performed using GenomeStudio V2.0.5 implemeting GenTrain Algorithmus 3.0 with a GenCall threshold of 0.2. All samples had call rates above 98%. Samples were tested for discordance between genetically inferred and annotated gender, and for genotype identity comparing genotypes by in-house scripts and by running the —genome computation implemented in plink v1.9. Genotype identity is assumed with less than 2% of genotypes not matching.

Declaration of Competing Interest

The authors declare that they have no known competing financial interests or personal relationships that could have appeared to influence the work reported in this paper.

Acknowledgments

This work was supported by ERA-NET NEURON under Grant No. 01EW1902 (DECODE!), the Horizon 2020 Research and Innovation Programme under Grant No. 728018 (Eat2beNICE) and the 5-100 Russian Academic Excellence Project. This publication was supported by the Open Access Publication Fund of the University of Würzburg. G.C. Z. is supported by a grant from the DFG (Project No. 413657723 Clinician Scientist-Program UNION CVD). We thank Julia Merk, Nicole Schraut, and Gabriela Ortega for excellent technical assistance.

Appendix A. Supplementary data

Supplementary data to this article can be found online at https://doi.org/10.1016/j.scr.2021.102526.

References

Merker, S., Reif, A., Ziegler, G.C., Weber, H., Mayer, U., Ehlis, A.C., Conzelmann, A., Johansson, S., Müller-Reible, C., Nanda, I., Haaf, T., Ullmann, R., Romanos, M., Fallgatter, A.J., Pauli, P., Strekalova, T., Jansch, C., Vasquez, A.A., Haavik, J., Ribasés, M., Ramos-Quiroga, J.A., Buitelaar, J.K., Franke, B., Lesch, K.P., 2017. SLC2A3 single-nucleotide polymorphism and duplication influence cognitive processing and population-specific risk for attention-deficit/hyperactivity disorder. J. Child. Psychol. Psychiatry. 58 (7), 798–809. https://doi.org/10.1111/jcpp.12702. Epub 2017 Feb 22 PMID: 28224622.

Mlynarski, E.E., Sheridan, M.B., Xie, M., Guo, T., Racedo, S.E., McDonald-McGinn, D.M., Gai, X., Chow, E.W., Vorstman, J., Swillen, A., Devriendt, K., Breckpot, J., Digilio, M. C., Marino, B., Dallapiccola, B., Philip, N., Simon, T.J., Roberts, A.E., Piotrowicz, M., Bearden, C.E., Eliez, S., Gothelf, D., Coleman, K., Kates, W.R., Devoto, M., Zackai, E., Heine-Suñer, D., Shaikh, T.H., Bassett, A.S., Goldmuntz, E., Morrow, B.E., Emanuel, B.S., International Chromosome 22q11.2 Consortium, 2015. Copy-number variation of the glucose transporter gene SLC2A3 and congenital heart defects in the 22q11.2 deletion syndrome. Am. J. Hum. Genet. 96 (5), 753–764. https://doi.org/10.1016/j.ajhg.2015.03.007. Epub 2015 Apr 16. PMID: 25892112; PMCID: PMC4570279.

Prakash, S.K., Bondy, C.A., Maslen, C.L., Silberbach, M., Lin, A.E., Perrone, L., Limongelli, G., Michelena, H.I., Bossone, E., Citro, R., BAVCon Investigators, GenTAC Registry Investigators, Lemaire, S.A., Body, S.C., Milewicz, D.M., 2016. Autosomal and X chromosome structural variants are associated with congenital heart defects in Turner syndrome: The NHLBI GenTAC registry. Am. J. Med. Genet. A 170 (12), 3157–3164. https://doi.org/10.1002/ajmg.a.37953. Epub 2016 Sep 8. PMID: 27604636; PMCID: PMC5115959.

Vittori, A., Breda, C., Repici, M., Orth, M., Roos, R.A., Outeiro, T.F., Giorgini, F., Hollox, E.J., 2014. REGISTRY investigators of the European Huntington's Disease Network. Copy-number variation of the neuronal glucose transporter gene SLC2A3 and age of onset in Huntington's disease. Hum. Mol. Genet. 23 (12), 3129–3137. https://doi.org/10.1093/hmg/ddu022. Epub 2014 Jan 22. PMID: 24452335; PMCID: PMC4030768.

Ziegler, G.C., Almos, P., McNeill, R.V., Jansch, C., Lesch, K.P., 2020. Cellular effects and clinical implications of *SLC2A3* copy number variation. J. Cell. Physiol. 235 (12), 9021–9036. https://doi.org/10.1002/jcp.29753. Epub 2020 May 5 PMID: 32372501.